Accepted Manuscript

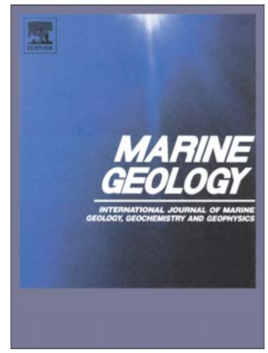

High-resolution seismic stratigraphy and morphology of the Scan Basin contourite fan, southern Scotia Sea, Antarctica

Marga García, Francisco J. Lobo, Andrés Maldonado, F. Javier Hernández-Molina, Fernando Bohoyo, Lara F. Pérez

PII: S0025-3227(16)30011-1
DOI: doi: 10.1016/j.margeo.2016.01.011
Reference: MARGO 5412

To appear in: *Marine Geology*

Received date: 1 June 2015
Revised date: 30 December 2015
Accepted date: 25 January 2016

High-resolution seismic stratigraphy and morphology of the Scan Basin contourite fan, southern Scotia Sea, Antarctica

Marga García[1,2,*], Francisco J. Lobo[1], Andrés Maldonado[1], F. Javier Hernández-Molina[3], Fernando Bohoyo[4], Lara F. Pérez[5]

(1) Instituto Andaluz de Ciencias de la Tierra, CSIC-Universidad de Granada. Avenida de las Palmeras 4, 18100 Armilla, Spain (*Corresponding autor: m.garcia@csic.es and marguita.garcia@gmail.com; pacolobo@iact.ugr-csic.es; amaldona@ugr.es)
(2) Renard Centre of Marine Geology, Ghent University, Krijgslaan 281 S8, B-9000 Gent, Belgium
(3) Department of Earth Sciences, Royal Holloway University of London, Egham, Surrey TW20 0EX, UK (javier.hernandez-molina@rhul.ac.uk)
(4) Instituto Geológico y Minero de España, Ríos Rosas, 23, 28003 Madrid, Spain (f.bohoyo@igme.es)
(5) Geological Survey of Denmark and Greenland, Geophysical Department, Øster Volgade 10, DK-1350 Copenhagen K, Denmark. (lfp@geus.dk and larafperez@gmail.com)

Abstract

The Scan Basin is the easternmost of the southern Scotia Sea basins. It is located in a complex tectonic setting, north of the boundary between the Scotia and Antarctic plates. In addition, Scan Basin is directly to the north of Bruce Passage, which connects the Scotia and Weddell seas through the northward overflow of the Weddell Sea Deep Water (WSDW). Scan Basin has been described as an isolated small oceanic basin, where the fan-shaped abyssal plain is bounded by Bruce and Discovery banks. Sedimentary processes involved in the development of the Scan Basin sediment record during the late Pliocene-Quaternary are discussed here, through the examination of the distribution and morphological and acoustic characteristics of erosional, depositional, gravitational, fluid-escape, and volcanic features in correlation to the geological and oceanographic setting. The abyssal plain reflects the action of high-energy bottom-current circulation along its western side and lower-energy bottom currents along the eastern side. In contrast, Discovery Bank reflects a highly dynamic interplay between bottom-current activity, mass-wasting processes, and processes linked to the water mass interfaces. Variations in the abyssal plain stratigraphy are associated with events that may be related to climate changes since the late Miocene, involving increased bottom-current circulation and variations in the interaction between the WSDW and the Antarctic Circumpolar Current. The Scan Basin sector is one example of a contourite depositional system developed downstream of a deep gateway exit, and its major depositional characteristics allow its classification as a contourite fan. These new findings contribute to clarifying the development of contourite fans in regions of significant bottom-water interchange.

Keywords: Scotia Sea; seafloor morphology; seismic stratigraphy; bottom-current circulation; contourite fan

1. Introduction

Contourite depositional and erosional processes reflect the influence of bottom currents in deep-sea environments. They have been the focus of extensive attention in recent decades due to their scientific, social, and economic relevance as they constitute targets for palaeoclimatology and palaeoceanography studies, geological hazard assessment, and hydrocarbon exploration (Rebesco et al., 2014). Several classifications of contourite erosional and depositional morphologies have been proposed (Faugères et al., 1993, 1999; Rebesco and Stow, 2001; Stow et al., 2002; Faugères and Stow, 2008; Hernández-Molina et al., 2008b; Rebesco et al., 2014). Contouritic features have been associated into Contourite Depositional Systems (CDS) and Complexes (Hernández-Molina et al., 2008a; Rebesco and Camerlenghi, 2008). Of the variety of contourites defined in the literature probably the least studied is the contourite fan, of which the Vema Fan is the best-known example (Faugères et al. 1993; Mézerais et al. 1993; Faugères et al. 1998). This fan is a cone-shaped sedimentary body deposited by the activity of the Antarctic Bottom Water (AABW) downstream of the Vema Channel exit in the southeast Brazilian Basin (Faugères et al. 1993). It is bounded by two major contourite channels, along which main cores of the bottom-water masses flow with the highest intensity, generating widespread erosion. The Sunda Basin drift (Sunda forearc region, Indonesia) shares some of the large-scale geomorphological patterns of contourite fans, although it has been defined as a confined sediment drift (Reed et al., 1987). It is composed of a central mound laterally bounded by base-of-slope channels related to the Pacific Ocean Deep Water flow. A contourite fan in the Scotia Sea has more recently been studied in detail and has revealed the interaction between the Weddell Sea water masses and the Antarctic Circumpolar Current (Maldonado et al., 2003; Hernández-Molina et al., 2008b), but high-resolution analysis focusing on the sedimentary processes and their relation with present oceanographic processes are still relatively scarce on contourite fans.

Scan Basin is one of the small basins through which the Weddell Sea Deep Water (WSDW) flows from the Weddell Sea to the Scotia Sea. The WSDW is involved here in the deposition of a complex contourite system, including a contourite fan, as it interacts with the Antarctic Circumpolar Current (ACC). The study of this system has provided important evidence of the regional palaeoceanographic evolution in relation to the opening of the Drake Passage (Maldonado et al., 2003; Hernández-Molina et al., 2007). Although the influence of the ACC flow in sedimentation has been demonstrated in other regions of the Scotia Sea based on high-resolution profiles (Owen et al., 2014), the Scan Basin stratigraphy has been mostly studied from multi-channel seismic profiles that allowed establishing its tectonic development and sedimentation since the opening of the basin (Hernández-Molina et al. 2007; Pérez et al., 2014a,b). In this work we characterize in detail the Scan Basin contourite features based on high-resolution datasets with two main objectives: 1) to determine the role played by sedimentary and oceanographic processes -and their interaction- in the Late Pliocene-Quaternary evolution of the Scan Basin; 2) to provide a high-resolution approach to the study of contourite fans in order to improve conceptual diagnostic features of these depositional systems.

2. Geological and oceanographic framework

2.1. Scan Basin in the context of the Scotia Arc

Scan Basin is the easternmost of a series of small basins in the southern Scotia Sea, north of the South Scotia Ridge (SSR) and including, from west to east: the Ona, Protector, Dove, and Scan basins (Fig. 1; British Antarctic Survey, 1985; Maldonado et al., 1998; Bohoyo et al., 2007; Galindo-Zaldívar et al., 2002, 2006; Lodolo et al., 2006, 2010; Maldonado et al., 2015). The SSR constitutes the plate boundary between the Scotia and Antarctic plates. Present-day tectonic activity is characterized by sinistral transcurrent motion along continental blocks of the SSR as revealed by the distribution of earthquake epicentres (Balanyá et al. 1999; Galindo-Zaldívar et al., 2002; Bohoyo et al. 2007). Bruce Passage forms a gateway through the SSR that connects Jane Basin in the Antarctic Plate with Scan Basin in the Scotia Plate. The passage is 3,000 m deep and is constricted to the east by a WNW-ESE-oriented basement high (Fig. 1b; Bohoyo et al., 2002; Hernández-Molina et al., 2007; Lodolo et al., 2010).

Laterally, Scan Basin is bounded by Bruce Bank to the west and by Discovery Bank to the east, and opens to the Scotia Sea to the north. The banks are mainly fragments of thinned continental crust dispersed throughout the southern sector of the Scotia Arc after the opening of Drake Passage. This opening occurred during the Eocene–Oligocene and led to the connection of the Pacific and the Atlantic oceans (Barker, 2001; Lawver and Gahagan, 2003; Maldonado et al., 2006; Livermore et al., 2007; Dalziel, 2013; Eagles and Jokat, 2014; Maldonado et al., 2014). The Scan Basin is mainly floored by oceanic crust and has ENE- to NNE-trending sinistral transcurrent faults in the southern basin that become NNW-oriented to the north (Pérez et al., 2014a). These features have been related with the opening of the basin that led to the separation of Bruce and Discovery banks (Lodolo et al., 2010; Civile et al., 2012), probably coevally with the opening of Drake Passage (Pérez et al., 2014a).

2.2. Oceanography

The Scotia Sea region is dominated by thermohaline circulation, of which Antarctica is the major contributor in the global circulation scheme (Speer et al., 2000; Morozov et al., 2010). Generally, the most prominent oceanographic feature is the ACC, which propagates from west to east around the Antarctic continent with relatively warm, saline water. It is composed of three fronts (Sub-Antarctic, Polar and Southern fronts, from north to south) and in the Scotia Sea it is strongly affected by the seafloor topography (Tarakanov, 2012).

In the Scotia Sea, the shallowest water mass is the Antarctic Surface Water (AASW; Naveira Garabato et al., 2002a). Below, the Circumpolar Bottom Water (CBW) and the Warm Deep Water (WDW) occupy the same depths, but the WDW is south of 58–59ºS (Fig. 2a; Naveira Garabato et al., 2002a). The CBW is the densest portion of the Circumpolar Deep Water (Orsi et al., 1999; Morozov et al., 2010), which constitutes the main component of the eastward-flowing ACC (Locarnini et al., 1993; Palmer et al., 2012). In the Scotia Sea the dominant water mass below the CBW is the Antarctic Bottom Water (AABW), originating mainly in the Weddell Sea and Ross Sea which includes the Weddell Sea Deep Water (WSDW). The WSDW comprises the upper and lower fractions (UWSDW and LWSDW, respectively; Fig. 2). It passes through Jane Basin and flows towards the Scotia Sea through four passages along the SSR: Phillip, Orkney, Bruce, and Discovery (Naveira Garabato et al., 2002). These passages contribute to the net transport of 15 ± 7 Sv over the SSR (Jullion et al., 2014). The WSDW flow across the South Scotia Ridge has been defined as a deep overflow that involves dense water mass undergoing mixing with overlying water as it escapes through a confining topographic barrier (Legg et al., 2009). A branch of the WSDW spreads westwards along the northern slopes of the South Scotia Ridge and reaches the Antarctic Pacific margin (Orsi et al., 1999; Naveira-Garabato et al., 2002). The upper boundary surface of the WSDW, which limits this water mass with the WDW/CBW, deepens along the Scotia Sea from about 1,500 m close to the SSR (Fig. 2a) to more than 3,500 m in the northern regions (Morozov et al., 2010). Regional circulation studies suggest that the CBW and the WDW have a general westward flow along the northern flank of the South Scotia Ridge, with southward recirculation within the small basins, whereas the WSDW flows mostly north to northwest through the basins (Morozov et al., 2010; Tarakanov, 2010). Some authors propose that the re-circulation pattern also affects the deep water masses, as revealed by lowered Acoustic Doppler Current Profiler (LADCP) data and numerical simulations (Naveira Garabato et al., 2002b; Schodlok et al. 2002; Jullion et al., 2014).

In Scan Basin, the shallowest water column is characterized by the AASW flowing with the ACC down to depths of around 150 m (Fig. 2b). The northernmost Discovery Bank is influenced by the CBW (Fig. 2; Naveira Garabato et al., 2002; Schodlok et al. 2002; Jullion et al., 2014). The deepest areas of the basin are affected by the upper and lower WSDW, at depths of over 2,000 m. Although the circulation pattern in Bruce Passage is not well known (Franco et al., 2007), general models indicate that re-circulation affects the water masses throughout the entire water column (Fig. 2b), with a northward western flow with velocities up to 15 cm s^{-1} and a weaker southward eastern flow with maximum velocities of 5 cm s^{-1} (Naveira Garabato et al., 2002b).

2.3. Stratigraphy and morphogenetic processes

Recent studies of the Scan Basin reveal a stratigraphic architecture that includes seven seismic units overlying the acoustic basement, which is interpreted as oceanic crust in the northern part of the basin (Pérez et al., 2014a). Ages were attributed based on the magnetic anomalies of the igneous oceanic crust and on estimated sedimentation rates in the Scotia Sea, and the sedimentary infilling of the basin is proposed to have started in the Oligocene, at about 26 Ma (Pérez et al., 2014a). During the first stage (probably coeval with the opening of Drake Passage), the basin's growth pattern was heavily influenced by mass transport processes (Pérez et al., 2014a). The sedimentary record suggests that it was followed by mainly oceanographically controlled sedimentation starting after the opening of gateways to the Weddell Sea from the middle Miocene (Bohoyo et al., 2002; Hernández-Molina et al., 2007; Pérez et al., 2014). This second phase of Scan Basin's evolution was, in contrast, largely controlled by the northward flow of deep waters from the Weddell Gyre through Jane Basin to the Scotia Sea (Maldonado et al., 2003; Hernández-Molina et al., 2007, 2008a; Pérez et al., 2014). The most recent seismic units of middle Miocene to Present-day age constitute a large contourite fan where numerous erosional features suggest intensified WSDW activity and a northward migration of the deposits (Pérez et al., 2014a). The northern area includes a complex system of depositional and erosional contourite features in the Scotia Sea that reflects the interaction between the WSDW and the ACC (Maldonado et al. 2003; Hernández-Molina et al. 2007).

Studies on the present-day morphology have revealed erosional furrows in the southwestern sector of the Scan Basin resulting from the interaction of the WSDW with a set of conjugate strike-slip faults (Lobo et al., 2011) and reflecting the activity of fluid-escape processes (Somoza et al., 2014). In the northern part of the Scan Basin, the Weddell Channel is a main feature in the Scotia Sea contourite depositional system (Maldonado et al., 2003). Other recent processes include frequent mass-transport (Ruano et al., 2014) and gas seepage that have produced numerous craters on the western flank of the Discovery Bank (Somoza et al., 2014).

3. Methods and Dataset

This work is based on geophysical databases collected on board the RV Hesperides during the SCAN cruises since 1997, including swath bathymetry and very high-resolution seismic reflection data. Swath bathymetric data were obtained with EM 12 and EM 120 SIMRAD™ systems. The equipment was operated at a frequency of 12 kHz and a swath aperture of 120°, obtaining seafloor coverage of about 3.5 times the water depth. Multibeam files were post-processed with NEPTUNE™ and CARIS™ software. Datasets have been displayed and interpreted using Fledermaus™ and Global Mapper™ software. Regional bathymetric data have been obtained from compilations of global seafloor bathymetry (Smith and Sandwell, 1997; Ryan et al., 2009). About 5000 km of very high-resolution seismic profiles were acquired using a TOPAS PS 18 system, operating in high-penetration (chirp) mode with a primary frequency of 18 kHz and up to 30 kW power. The acquired signal was post-processed (band-pass filters to reduce noise-to-signal ratio, bottom tracking, time variable gain, swell filter, stacking, muting, and delay correction) using TOPAS™ and Radexpro™ software. The resulting SEG-Y files were imported into a Kingdom Suite™ project for interpretation. The acoustic facies analysis is based on the combination of an echo-facies study following the criteria first proposed by Damuth (1980) and further developed by Kuhn and Weber (1993) and Droz et al. (2001), and a seismic facies analysis of attributes including the acoustic amplitude, lateral continuity, geometry, and internal configuration of reflections (Payton, 1977; Veeken, 2007).

4. Results

4.1. Physiographic Characterization

The Discovery and Bruce banks constitute large morphological highs, averaging 1,600–2,000 m water depth, but with several isolated reliefs as shallow as 600 m (Fig. 1b). Both banks are oriented roughly SW-NE, but Discovery Bank is fragmented into two blocks by a gap (hereafter Discovery Gap), and the northern block trends SSE-NNW. A narrow, steep slope (5–25 km wide, up to 15º steep) connects the shallow banks to the Scan Basin abyssal plain. Discovery Gap is about 30 km wide at depths of about 2,100 m and from there a 40 km wide relatively flat terrace at depths of about 2,200 m opens to the deep Scan Basin to the southwest. A smooth, 100 km wide ramp connects the terrace to the abyssal plain, forming a base-of-slope domain (Fig. 1b).

The Scan Basin abyssal plain is fan-shaped and widens from about 55 km in the proximal (southern) area of Bruce Passage up to 180 km at the northern opening to the Scotia Sea. The relatively flat seafloor has gradients generally under 0.5º, dipping NW at depths of 2,800–3,100 m. It is interrupted by isolated elevations less than 150 m high. In the central area, the transversal profile is asymmetrical, with maximum depths in the western basin. The distal part of the Scan Basin connects to the central Scotia Sea through the Weddell Channel (Fig. 1b).

4.2. Morphological and Acoustic Characterization of the Scan Basin

This study is based on the analysis of the bathymetry and high-resolution seismic profiles, which have allowed differentiating three acoustic facies (Fig. 3). Non-penetrative facies (I) are characterized by a high-amplitude seafloor reflection and the lack of penetration of the acoustic signal. It includes a Regular non-penetrative subtype (IA) showing a regular high-amplitude seafloor reflection. The Hyperbolic non-penetrative facies (IB) is characterized by diffractions of the non-penetrative seafloor reflection. Stratified facies (II) present layered reflections with medium to very high acoustic amplitude and very high lateral continuity. They occur as Parallel stratified facies (IIA) or Wavy stratified facies (IIB). Transparent acoustic facies (III) characterize irregular-to lens-shaped deposits with no internal reflections that occur either on the seafloor or in the subsurface.

The morphological and acoustic characterization allows identifying a series of features that are classified as erosive (lineations, dendritic channels, furrows, and channels), depositional (sheeted deposits, sediment waves, and mounded bodies), gravitational (scarps, irregular or lens-shaped transparent bodies), related to fluid escape (craters) and volcanic features (Fig. 4).

Lineations and dendritic channels are the main erosional features in the Bruce Passage area (Fig. 4). *Lineations* form a series of SSE-NNW and WSW-ENE oriented ridge-and-channel morphologies with reliefs of up to 100 m (Fig. 5b). *Dendritic channels* are narrow depressions up to 30 km long, 40 m deep, and 1 km wide with a general NE-SW convergent dendritic pattern (Fig. 4). Both lineations and dendritic channels display hyperbolic non-penetrative acoustic facies (IB). To the north of Bruce Passage the predominant erosional features are the N–NNW or NE-oriented *furrows* previously described by Lobo et al. (2011) and Somoza et al. (2014). Furrows in the western part are relatively straight and elongated (up to 20 km long and 1–2 km wide) with abrupt flanks some tens of metres high (Fig. 5c). In contrast, furrows in the eastern part are generally shorter, wider (up to 8 km long and 2–3 km wide), and smoother in relief, generally less than 50 m deep. Some have been partially or totally infilled by the most recent sedimentation (Fig. 5d). Furrows have wavy acoustic facies (IIB). *Channels* occur along the margins of the abyssal plain, around isolated morphological highs, and in the Discovery Bank area (Figs. 4 and 6). Along the margins of the abyssal plain channels display sinuous patterns, parallel to the bank flanks (Fig. 4). They are up to 40 km long, 2–3 km wide, and up to 100 m deep. The deeper channels occur in the distal regions of the abyssal plain, where they connect with the Weddell Channel (Figs. 6i and 6j). Channels around isolated reliefs on the abyssal plain have a similar morphology but are more deeply incised along the western side of the reliefs (Figs. 6j and 6l). Channels on the Discovery Bank terrace are up to 100 m deep and 2–3 km wide and display high sinuousity (Fig. 4). A major channel, about 80 m deep and 3 km wide, has truncated reflections on its eastern flank and can be traced for more than 50 km (Fig. 6k). The base-of-slope area is limited laterally by two small channels, less than 20 m deep (Fig. 6m). In general, the channel thalwegs have regular non-penetrative (IA) or transparent (III) acoustic facies.

Depositional features include *sheeted deposits* on the abyssal plain where the parallel stratified acoustic facies (IIA) predominate (Fig. 5f). *Sediment waves* occur mostly on the eastern and distal abyssal plain, on part of the Discovery Bank terrace, and on the central part of the base-of-slope (Fig. 4). They are a few metres high with crests up to 20 km long oriented WSW-ENE in proximal areas that become more irregular towards the distal part of the abyssal plain (Fig. 4). They have wavy stratified acoustic facies (IIB; Figs. 5g and 5h). *Mounded bodies* are generally associated to channels along the margin and around isolated reliefs on the abyssal plain and on Discovery Bank (Fig. 4). They are generally small and irregular (20–50 m high) on the abyssal plain, where they form parallel, multi-crested features (Figs. 4, 5, and 6). In the Discovery Bank area, they are up to 300 m high and 40 km long and are associated to channels and morphological highs (Fig. 4). Mounded bodies display parallel to wavy stratified acoustic facies (IIA and IIB) where reflections generally prograde towards the channels (Fig. 5g and 5k), except for a body on the Discovery Bank terrace that displays truncated reflections at the channel flank (Fig. 6k).

Gravitational features include scarps and transparent bodies that mostly occur on the flanks and foot of the Bruce and Discovery banks (Fig. 4). *Scarps* are particularly common on the flanks of the distal Discovery Bank (Figs. 4 and 7). Individual scarps are typically less than 10 km long and delimit steep ramps of up to 7º. Scarps are generally amphitheatre-shaped in plain view and tend to coalesce, especially at the distal part of the banks. Many large scarps are composed of laterally connected smaller semi-circular scarps between 1 and 3 km in diameter (Fig. 7d). They also occur at different depths, producing a step-like profile of the bank flanks and some of the wider scarps include smaller ones within them. The areas affected by scarps display regular or hyperbolic non-penetrative acoustic facies (IA, IIB). Irregular or lens-shaped *transparent bodies* are widely distributed at the foot of slopes on the bank flanks (Figs. 4 and 7b). They are most frequent at the foot of Discovery Bank, but are also found at the foot of isolated reliefs.

Transparent bodies occur on the surface but also in the sub-surface record, interbedded within mounded bodies at the margins of the abyssal plain (Figs. 4, 7n).

Fluid-escape features include the *craters* described by Somoza et al. (2014) on Discovery Bank. They occur at depths averaging 2,100 m (Fig. 7d) and have circular to elliptical shape with diameters of 0.3–2.5 km and depths of up to 200 m. They occur generally as isolated features although in some cases they may result from the amalgamation of several craters, particularly in the eastern part of the study area. They are especially common on the top of mounded bodies, but absent in the thalweg and channel rims. The area affected by craters has wavy stratified facies (IIA). The *volcanic features* comprise numerous cone-shaped morphological highs in the two blocks of Discovery Bank (Fig. 4). They have diameters of 10–15 km and heights of up to 800 m. They display hyperbolic non-penetrative acoustic facies (IB) on their top and stratified facies (IIA and IIB) on their flanks.

4.3. High-resolution seismic stratigraphy

Based on the analysis of the TOPAS profiles, five seismic units have been identified in the central and distal areas of the Scan Basin abyssal plain. They lie within the younger Seismic Unit I, of late Pliocene-Quaternary age of Pérez et al. (2014a) and are named U5 to U1 from older to younger (Figs. 8a and 8b). Seismic units mostly exhibit parallel or wavy stratified acoustic facies (IIA and IIB) with very high continuity along the entire basin floor. They have erosional limits at the margins of the abyssal plain, often related with transparent bodies that become generally conformable throughout the rest of the abyssal plain. Seismic unit U5 is relatively thin, with a maximum thickness of about 40 ms in a depocenter in the distal deepest part of the basin and less than 15 ms in the rest of the area (Fig. 8c). Seismic unit U4 has two main depocenter on the western and eastern sides of the abyssal plain (maximum thickness of 34 ms) and a secondary depocenter of about 20 ms in a more proximal basin location. Seismic unit U3 shows a maximum thickness of about 60 ms in the distal part of the abyssal plain and an area of low thickness in the eastern part (Fig. 8c).

Seismic units U2 and U1 have some differential characteristics compared with the older U5-U3 seismic units (Figs. 8d and 8e). The differences include: 1) A marked increase in seismic amplitude. 2) A change in the distribution pattern. Seismic units U2 and U1 have significantly greater thickness that progressively increases towards the distal areas, where they reach values of more than 150 ms. They display marked lateral changes along the units (particularly in the vicinity of depressions) and they exhibit patchy distribution in the distal and marginal parts of the abyssal plain. 3) A change in the depositional style in the furrows region, from an erosional character represented by units U5 to U3 to the partial or total infilling of most of these features by units U2 and U1 (Fig. 8d). The present-day mounded topography is also attributed to seismic units U2 and U1, which also display a more marked progradational configuration in the mounded bodies (Fig. 8). And 4) the base of the two most recent seismic units at the margins of the abyssal plain show a more pronounced erosional character than the older ones, locally characterized by a very high acoustic amplitude reflector (Fig. 8e). It is often associated with lens-shaped or irregular bodies of transparent facies at the margins of the abyssal plain. Although U2 and U1 have similar seismic characteristics compared to the older seismic units, they are separated by a discontinuity that marks an internal increase in acoustic amplitude and is laterally correlated with the base of transparent bodies at the limits of the abyssal plain. Differences in terms of the migration of wavy reflections and the occurrence of acoustic blanking features can also be identified in the two subunits (Fig. 8e). They have similar thickness, but subunit U1 displays a more distinct patchy distribution along the distal abyssal plain (Fig. 8c).

5. Discussion

5.1. *Interpretation of the morphological features: Sedimentary processes*

The physiography of the Scan Basin is a fan-shaped abyssal plain bounded by the steep, narrow slopes of Bruce and Discovery banks in the central Scotia Sea and isolated from any major source of continental sediment input (Fig. 1). The general absence of a well-developed base of slope/continental rise domain suggests the relatively slight influence of downslope depositional processes in the recent evolution of the Scan Basin. Mass-wasting processes derived from the continental margins of the Antarctic Peninsula largely occurred during the initial phases of development, when the basin was located in a westward position before the middle Miocene (Pérez et al., 2014a). Since then, the WSDW flow has dominated sedimentation in the basin (Hernández-Molina et al., 2007; Pérez et al., 2014a). The base-of-slope off Discovery Gap likely results from a relatively high occurrence of mass-wasting processes favoured by seismic activity caused by the abundant volcanic edifices in the region (Fig. 4).

The distribution of morphological features in the Scan Basin allows the distinction of two regions: (1) the *abyssal plain*, dominated by erosional features in the proximal Bruce Passage area, depositional features in the central part, and associations of erosional and depositional features along the margins; and (2) the *banks*, characterized by an irregular physiography, a relatively thinner sediment drape, and an abundance of volcanic edifices and fluid-escape features (Figs. 4 and 7). The two regions are connected by the slopes, which are mostly characterized by gravitational features. The late Pliocene-Quaternary sedimentary evolution of these two regions reflects the action of bottom currents, and their depositional and erosional features are interpreted according to the nomenclature proposed by McCave and Tulholke (1986), Faugères et al. (1999), and reviewed by Rebesco et al. (2014).

5.1.1. The abyssal plain

The proximal region within the abyssal plain reflects the action of high-energy bottom current circulation as it is characterized by hyperbolic non-penetrative acoustic facies (Mézerais et al., 1993; Faugères et al., 2002) that are the result of a reduced sedimentary cover (Fig. 8) and the excavation of lineations and dendritic channels (Fig. 4). The channels and associated mounded deposits in the central and marginal areas are interpreted as contourite moats and mounded drifts. Moats are eroded by bottom currents along the foot of the slopes (left-hand side of the current) and mounded drifts are deposited along its right-hand flank due to the decrease in velocity and the effect of the Coriolis force influencing the migration of flows in a leftward direction for the Southern Hemisphere (Mougenot and Vanney, 1982; Gonthier et al., 1984; Faugères and Stow, 1993; Faugères et al., 1993, 1999). Furrows are indicators of the erosional activity of bottom currents and are initiated by helical secondary circulation in the bottom layers, being later eroded by current flows within the incipient depressions (e.g. Flood, 1994). Erosional furrows in the Scan Basin western abyssal plain (Figs. 4 and 5) result from the interaction between a northward-flowing bottom current and the scarps of the strike-slip faults (Lobo et al., 2011). The NNE trend of furrows, oblique to the current flow, points to the erosional activity of small current filaments detached from the main flow towards its right-hand side within the bottom Ekman layer (Pedlosky, 1996), as inferred from similar furrows identified in the Gulf of Cádiz as erosional products of the Mediterranean Outflow Water (Hernández-Molina et al., 2014). The location of furrows has alternatively been related to fluid-venting structures (Somoza et al., 2014). This type of feature is also prone to be progressively deformed from crater-like depressions into elongated depressions by the reworking effect of bottom currents (Bøe et al., 1998; Andresen et al., 2008). Furrows in the eastern Scan Basin (Figs. 4 and 5) likely result from the activity of flow filaments detached from a south-westward-flowing current of lower velocity, as suggested by their less consistent trend and size (Lobo et al., 2011). The stratified deposits in the central sector of the abyssal plain (Figs. 4 and 6) are interpreted as sheeted drifts. These drifts reflect a lower-energy environment (Mézerais et al., 1993; Faugères et al., 1998; 2002) and suggest the activity of currents flowing as tabular water masses throughout most of the central abyssal plain (Hernández-Molina, 2008). The irregularity of the sediment waves, their crest orientation, and their asymmetry suggest a bottom current-related origin (Wynn and Stow, 2002).

5.1.2. The banks region

Discovery Bank is characterized by isolated volcanic edifices (Fig. 4) that are part of the widespread volcanic manifestations that affect the entire bank (Vuan et al., 2005; Pérez et al., 2014a). Shallow areas are dominated by sheeted drifts in the flat central areas and by channels and associated mounded deposits interpreted as contourite moats and drifts (Faugères et al., 1993, 1999). Channels around the volcanic edifices develop as contourite moats related to the complex interaction of bottom currents around isolated obstacles (Roberts et al., 1974; McCave and Carter, 1997; Hernández-Molina et al., 2006). The sheeted deposits on the base-of-slope that evolve laterally to mounded deposits limited by channels (Fig. 6f) are interpreted as confined drifts, whereas the stratified deposits on the slope form a plastered drift attached to the flank of the bank (Rebesco et al., 2014).

Craters in Discovery Bank (Fig. 7) reflect fluid-escape processes in an area where bottom simulating reflectors (BSRs) have been recognized suggesting the presence of gas hydrates and diagenetic processes (Somoza et al., 2014), while widespread slope instability is suggested by the abundant scarps and transparent bodies on the bank flanks (Figs. 6 and 7) that constitute mass transport deposits (MTDs; Ruano et al., 2014). Instabilities may be related to the character of contourite sediments due to factors including the low shear-strength of deposits, under-consolidation and excess pore pressure, loading and gas charging, and the seabed-smoothing effect of contourite deposition (Bryn et al., 2005; Laberg and Camerlenghi, 2008). The spatial distribution of craters and slide scarps (Figs. 7 and 9) points to a relationship between contourite sedimentation, fluid-venting processes, and sediment instability. The relatively high sedimentation rate related with contourite deposition may explain the occurrence of fluid-escape processes and the higher density of craters on the mounded drifts, since high sedimentation rates would favour fluid expulsion, creating mass defects under the seafloor followed by gravity collapse to generate the craters (Josenhans et al., 1978; Hovland, 1984; Gay, 2002). In contrast, the total absence of craters within contourite channels (Fig. 9a) results from lower sedimentation rates and/or the erosional activity of the currents reworking and eroding the fluid-venting structures, impeding their present-day morphological expression. A detailed analysis of the slide scars on Discovery Bank reveals that they are composed of small, amalgamated 1–2.5 km wide semi-circular scarps that strongly resemble the shape and dimensions of fluid-venting craters (Fig. 9b).

Slide scars mostly occur on the western flank of Discovery Bank, where very few present-day craters can be identified (Figs. 4 and 9). This suggests that craters have a major influence on the distribution of mass-wasting processes. The influence of fluid-escape processes on sediment stability has been established in different geological settings (Bayon et al., 2009; Plaza-Faverola et al., 2010; Frey-Martínez et al., 2011). The injection of escaping fluids into the sediment may increase pore pressure, but the craters themselves can form discontinuities of reduced shear resistance, promoting destabilization, even after fluid-seepage activity has ceased (Lastras et al., 2007). In addition to the fluid-escape control, other factors may contribute to failure in this area, including the steep slopes of the banks margins (Casas et al., 2004; Laberg and Camerlenghi, 2008), highly energetic oceanographic regime (see review in Rebesco et al., 2014; Hanebuth et al., 2015), and widespread seismicity associated to the intense deformation in the Scotia-Antarctica plate boundary region (Bohoyo et al., 2007; Pérez et al., 2014; Ruano et al., 2014). Moreover, as observed at the foot of Discovery Bank, the deposition of mass-wasting deposits modifies the geometry of the contourite deposits (Fig. 7b), which may affect bottom circulation, which tends to adapt to the newly generated topography.

5.2. The Scan contourite fan

The main deposits along the abyssal plain of the Scan Basin are interpreted as a contourite fan produced by the flow of the WSDW; it represents the most proximal depositional element of the important deep-water flow system of the Scotia Sea (Maldonado et al., 2003; Hernández-Molina et al. 2007). Figure 10 shows a sketch of the flow patterns affecting the seafloor as inferred from the high-resolution stratigraphic and morphological analysis. The WSDW flow is enhanced as it crosses Bruce Passage (Hernández-Molina et al., 2007; Maldonado et al., 2003; Tarakanov, 2009; Morozov et al., 2010; Pérez et al., 2014a) and is responsible for the proximal erosional features (Fig. 10). As it is affected by the Coriolis force, it generates the contourite moats and associated mounded drifts on the western side of the abyssal plain (Fig. 4). On the eastern side, in contrast, contourite moats and drifts are smaller and have less lateral continuity. In addition, erosion is less evident, all of which suggests a relatively less energetic south-westward current, consistent with the counter-current identified in the eastern Bruce Passage (Naveira Garabato et al., 2002a). This is also in agreement with the development of furrows as the result of the interaction of filaments of the bottom current with the seafloor (Figs. 4 and 10), which erodes deeper, NNE-trending furrows in the western part (WSDW main core) and smaller furrows on the eastern side. This may be related to the slower flow velocity (Lobo et al., 2011), but it could also reflect the higher variability affecting this type of counter-currents (Mézerais et al., 1993; Faugères et al, 1998, 2008; Morozov et al., 2010). The central abyssal plain is dominated by tabular, less-energetic flows (Pérez et al., 2014a) that result in the deposition of sheeted drifts and sediment waves (Fig. 4).

The distal contourite fan represents a more complex depositional setting (Fig. 4). The distal channels are connected to the Weddell Channel, which is related to the northward-flowing WSDW (Maldonado et al. 2003). In contrast, contourite moats and drifts along the foot of Discovery Bank and the asymmetry of channels surrounding isolated obstacles on the distal abyssal plain suggest an E- to SE-trending bottom current (Roberts et al., 1974; McCave and Carter, 1997; Hernández-Molina et al., 2008a; Hanebuth et al., 2015). Oceanographic models suggest that the abyssal plain is swept by WSDW flowing northward along the western basin and southward along the eastern basin (Fig. 2). We propose that in the distal part of the Scan Basin abyssal the WSDW is split into a main northward-flowing core that continues flowing toward the Scotia Sea and a weaker counter-current that flows southeast (Fig. 10). This weaker flow could be intensified by interaction with the steep flanks of Discovery Bank, thus generating the contourite moats and associated drifts. This complex circulation pattern may be responsible for the increasing variability of sediment waves (Stow et al., 2009) and for the complex contourite deposits, including multi-crested drifts (Stoker et al., 1998).

Discovery Bank includes landforms of contourite origin consistent with the circulation pattern of the generally eastward-flowing CBW/WDW that affect the shallow bank as they flow with the ACC (Figs. 2a and 10; Morozov et al., 2010; Tarakanov, 2010). The confined and plastered drifts on the base-of-slope connecting Discovery Bank with the abyssal plain also suggest a NE-trending deep flow, probably also related with the CBW/WDW (Fig. 10). In this area, the complex sedimentary pattern may be favoured by the high-energy depositional setting resulting from the interface-related processes at the transition zone between the CDW/WDW and the WSDW as it occurs in other areas where water masses circulation affects sedimentation (Hernández-Molina et al., 2009; Preu et al., 2013; Rebesco et al., 2014; Hanebuth et al., 2015).

5.3. Late Pliocene-Quaternary sedimentary evolution of Scan Basin

The five high-resolution seismic units defined in this study lie within the most recent low-resolution seismic unit, Seismic Unit I (Fig. 8) of Pérez et al. (2014a). Despite the lack of direct chrono-stratigraphic control this unit was attributed to late Pliocene-Quaternary to Present age (3.8-0 Ma) by correlation with the works of Maldonado et al. (2003, 2005, 2006b), based on estimations of magnetic anomalies of the igneous oceanic crust and on the sedimentation rates estimated in the Scotia Sea (Pérez et al., 2014a). Seismic Unit I has been interpreted as a massive, northward-migrating contourite fan deposited after the opening of Bruce Passage

(Hernández-Molina et al., 2007; Pérez et al., 2014a). The distinct stratigraphic changes observed between the older units U5 to U3 and the most recent units U2 and U1 are interpreted as being the result of changes in the bottom-current patterns. During deposition of seismic units U5 to U3, the WSDW would have affected the entire width of the basin, being less energetic and therefore less capable of producing significant erosion/deposition. In contrast, seismic units U2 and U1 reflect intensifications in the current flow, probably due to latitudinal displacements of the interphase between the WSDW and the ACC that enhanced the erosional capacity of this flow on the western side of the abyssal plain. This would have displaced the WSDW core towards Bruce Bank and allowed the formation of the recirculation core along the eastern margin of the basin. This almost cyclonic circulation pattern would produce flow concentration along the flanks of the banks, leaving a central region of reduced energy, displaced to the east of the basin, which also coincides with the base-of-slope domain. This scenario indicates that the characteristics of subunits U2 and U1 would indicate successive events of current intensification during the Late Pliocene-Quaternary. Although chronostratigraphic correlations are not possible in the high-resolution datasets interpreted in this study, these events may be related to climatic events since the late Miocene that affect the pattern of interaction with the ACC flow, involving increased bottom-current circulation and WSDW generation (Anderson and Shipp, 2001; Hillenbrand and Ehrmann, 2005).

5.4. The Scan contourite fan: Implications for sedimentary models

Deposits within the Scan Basin abyssal plain can be considered as a contourite fan, or a channel-related drift, developed downstream of a channel exit (Mézerais et al., 1993; Faugères et al., 1998; Faugères et al., 2002, 2008). The strong topographic control on deep-water circulation is the main characteristic of this type of contourite drifts (Reed et al., 1987; Mézerais et al., 1993; Faugères et al., 1998). Taking into account the basin evolution since the opening of the basin (Hernández-Molina et al., 2007; Pérez et al., 2014a), the contourite deposits in the Scan Basin share some of the diagnostic features of contourite fans: 1) association with deep-water channels or gateways through which bottom circulation is constrained, which leads to an increase in flow intensity and velocity; 2) similar size (a few hundreds of kilometres in width and radius); 3) a depositional stacking pattern characterized by vertical aggradation and a progradation of deposits towards distal positions from the exit of the gateway; and 4) an association of acoustic facies on the depositional body that indicates variations in deep-water current speed in different parts of the system. Nevertheless, the Scan Basin contourite fan has some differential characteristics since it is fed by the WSDW flowing through only one channel on the western side of the basin, whereas the eastern channel features are the result of local recirculation. Deposition in the abyssal plain would only be constrained by the topographical barriers of Bruce and Discovery banks, although a similar configuration to that of the Vema fan and Sunda drift occurs in distal regions, where channels develop at the foot of the two banks (Reed et al., 1987; Faugères et al. 1993; Mézerais et al. 1993; Faugères et al. 1998).

6. Summary and conclusions

Two distinct depositional systems are recognized in the Scan Basin in the late Pliocene-Quaternary record. The abyssal plain system is defined as a contourite fan that is the most proximal element of a major contourite depositional system related with the WSDW flow in the Scotia Sea. It is controlled by incursions of the WSDW, preferentially along the western side of the basin, and by its partial recirculation along the eastern side. The Discovery Bank system is more directly influenced by eastward flow of the CBW and WSDW. The distribution and characteristics of the morphological features composing these systems are defined by bottom-current activity and its interplay with seafloor topography, and also reflect the interaction between a suite of secondary phenomena, including mass wasting and fluid escape.

Shallow high-resolution stratigraphy of the Scan Basin indicates oceanographic changes during the late Pliocene-Quaternary, probably influenced by interaction between the Weddell and Scotia seawater masses. The study of these interactions based on high-resolution datasets provides valuable information on oceanographic and climate changes that affect global circulation. To further understand recent sedimentary and oceanographic changes and to integrate them with regional models of the Scotia Sea depositional history, more precise stratigraphic constraints should be established by chronological correlations with marine sediment cores in the Scan Basin. Characterization of the Scan Basin depositional system contributes to the knowledge of contourite fans, which have up to now been scarcely studied compared to other types of contourite systems, and demonstrates that a similar configuration to that of the classic models reflects a more complex oceanographic setting.

Acknowledgements

This work was funded through CTM2008-06386-C02/ANT, CTM2011-30241-C01/CO2 ANT and CTM2014-60451-C2-1/2P projects and partially related to the CTM2012-39599-C93 project. The research of Marga Garcia has been funded by a Juan de la Cierva Grant (Spanish Ministry of Economy and Competitivity) and a Talentia Grant (Junta de Andalucía and European Union, grant reference 267226) and belongs to the "Leyendas Urbanas" group (http://www.aacte.eu/wp/). Research was conducted in the framework of the Continental Margins Research Group of the Royal Holloway University of London. The English style of this manuscript was thoroughly revised by Christine Laurin.

Bibliography

Anderson, J.B., Shipp, S.S., 2001. Evolution of the West Antarctic ice-sheet, in: Alley, R.B., Bindschadler, R.A. (Eds.), The West Antarctic ice sheet: behavior and environment. AGU Antarctic Research Service 77, pp. 45–58.

Andresen, K.J., Huuse, M., Clausen, O.R., 2008. Morphology and distribution of Oligocene and Miocene pockmarks in the Danish North Sea—implications for bottom current activity and fluid migration. Basin Research, 20, 445–466.

Balanyá, J.C., Galindo-Zaldívar, J., Jabaloy, A., Leitchenkov, G., Maldonado, A., Rodríguez-Fernández, J., Vinnikovskaya, O., 1999. Structure of the South Powell Ridge (NE Antarctic Peninsula): new clues for changing tectonic regimes near the Scotia/Antarctica Plate boundary. Geo-Marine Letters 18, 215–224. doi:10.1007/s003670050071

Barker, P.F., 2001. Evolution of the Scotia Sea region: relevance to broad-band seismology. Terra Antarctica 8, 67–70.

Bayon, G., Loncke, L., Dupré, S., Caprais, J.-C., Ducassou, E., Duperron, S., Etoubleau, J., Foucher, J.-P., Fouquet, Y., Gontharet, S., Henderson, G.M., Huguen, C., Klaucke, I., Mascle, J., Migeon, S., Olu-Le Roy, K., Ondréas, H., Pierre, C., Sibuet, M., Stadnitskaia, A., Woodside, J., 2009. Multidisciplinary investigation of fluid seepage on an unstable margin: the case of the Central Nile deep sea fan. Marine Geology 261, 92–104.

Bøe, R., Rise, L., Ottesen, D., 1998. Elongate depressions on the southern slope of the Norwegian Trench (Skagerrak): morphology and evolution. Marine Geology 146, 191–203.

Bohoyo, F., Galindo-Zaldívar, J., Maldonado, A., Schreider, A.A., Suriñach, E., 2002. Basin development subsequent to ridge–trench collision: the Jane Basin, Antarctica. Marine Geophysical Researches 23, 413–421.

Bohoyo, F., Galindo-Zaldivar, J., Jabaloy, A., Maldonado, A., Rodríguez-Fernández, J., Schreider, A., Suriñach, E., 2007. Extensional deformation and development of deep basins associated with the sinistral transcurrent fault zone of the Scotia–Antarctic plate boundary, in: Cunningham, W.D., Mann, P. (Eds.), Geological Society Special Publication 290, pp. 203–217.

British Antarctic Survey, 1985; British Antarctic Survey, 1985. Tectonic map of the Scotia Arc, in: British Antarctic Survey, C., (Eds.), Sheet (Misc) 3, p. Scale 1:3.000.000.

Bryn, P., Berg, K., Stoker, M.S., Haflidason, H., Solheim, A., 2005. Contourites and their relevance for mass wasting along the Mid-Norwegian Margin. Marine and Petroleum Geology 22, 85–96

Casas, D., Ercilla, G., Estrada, F., Alonso, B., Baraza, J., Lee, H., Kayen, R., Chiocci, F., 2004. Physical and Geotechnical Properties and Assessment of Sediment Stability on the Continental Slope and Basin of the Bransfield Basin (Antarctica Peninsula). Marine Georesources and Geotechnology 22, 253–278.

Civile, D., Lodolo, E., Vuan, A., Loreto, M.F., 2012. Tectonics of the Scotia–Antarctica plate boundary constrained fromseismic and seismological data. Tectonophysics 550–553, 17–34.

Dalziel, I.W.D., 2013. Antarctica and supercontinental evolution: clues and puzzles. Earth and Environmental Science Transactions of the Royal Society of Edimburgh 104, 3–16.

Damuth, J.E., 1980. Use of high-frequency (3.5-12 kHz) echograms in the study of near-bottom sedimentation processes in the deep-sea: a review. Marine Geology 38, 51–75.

Droz, L., Kergoat, R., Cochonat, P., Berné, S., 2001. Recent sedimentary events in the western Gulf of Lions (Western Mediterranean). Marine Geology 176, 23–37.

Eagles, G., Jokat, W. 2014, 2014. Tectonic reconstructions for paleobathymetry in Drake Passage. Tectonophysics 611, 28–50.

Faugères, J.C., Stow, D.A.V., 1993, Bottom-current-controlled sedimentation: a synthesis of the contourite problem. Sedimentary Geology 82, 287–297

Faugères, J.C., Stow, D.A.V., 2008. Contourite drifts. Nature, evolution and controls, in: Rebesco, M., Camerlenghi, A. (Eds.), Developments in Sedimentology, vol. 60, pp. 259–288.

Faugères, J.C., Mézerais, M.L., Stow, D.A.V., 1993. Contourite drift types and their distribution in the North and South Atlantic Ocean basins. Sedimentary Geology 82, 189–203.

Faugères, J.-C., Imbert, P., Mézerais, M.L., Cremer, M., 1998. Seismic patterns of a 'contourite fan' – muddy drift related to the Vema Channel (South Brazilian basin) – and a sandy distal deep-sea fan downstream of the Cap Ferret system (Bay of Biscay): a comparison. Sedimentary Geology 115, 81–110.

Faugères, J.C., Stow, D.A.V., Imbert, P., Viana, A., 1999. Seismic features diagnostic of contourite drifts. Marine Geology 162, 1–38.

Faugères, J.C., Zaragosi, S., Mezerais, M.L., Masse, L., 2002. The Vema contourite fan in the South Brazilian basin, in: Stow, D.A.V., Pudsey, C.J., Howe, J.A., Faugères, J.C., Viana, A.R. (Eds.), Deep-Water Contourite Systems: Modern Drifts and Ancient Series, Seismic and Sedimentary Characteristics. Geological Society, London, Memoirs 22, pp. 209–222.

Flood, R.D., 1994. Abyssal bedforms as indicators of changing bottom current flow: Examples from the U.S. East Coast continental rise. Paleoceanography 9, 1049–1060.

Franco, B.C., Mata, M.M., Piola, A.R., Garcia, C.A.E., 2007. Northwestern Weddell Sea deep outflow into the Scotia Sea during the austral summers of 2000 and 2001 estimated by inverse methods. Deep-Sea Research I 54, 1815-1840.

Frey-Martínez, J., Bertoni, C., Gerard, J., Matías, H., 2011, In: R. Craig Shipp, Paul Weimer, Henry W. Posamentier (Eds.), Mass-transport Deposits in Deepwater Settings. SEPM Special Publication 96, Tulsa, Oklahoma, USA. 181-198.

Galindo-Zaldivar, J., Balanyá, J.C., Bohoyo, F., Jabaloy, A., Maldonado, A., Martínez-Martínez, J.M., Rodríguez-Fernández, J., Suriach, E., 2002. Active crustal fragmentation along the Scotia–Antarctic plate boundary east of the South Orkney Microcontinent (Antarctica). Earth and Planetary Science Letters 204, 33–46.

Galindo-Zaldivar, J., Bohoyo, F., Maldonado, A., Schreider, A., Suriñach, E., Vázquez, J.T., 2006. Propagating rift during the opening of a small oceanic basin: the Protector Basin (Scotia Arc, Antarctica). Earth and Planetary Science Letters 241, 398–412.

Gay, A., 2002. Les marqueurs géologiques de la migration et de l'expulsion des fluides sédimentaires sur le plancher des marges passives matures. Exemples dans le bassin du congo. PhD Thesis, Université des Sciences et Technologies de Lille.

Girton, J.B., Pratt, L.J., Sutherland, D.A., Price, J.F., 2006. Is the Faroe Bank Channel overflow hydraulically controlled?. Journal of Physical Oceanography 36, 2340–2349.

Gonthier, E., Faugères, J.-C., Stow, D.A.V., 1984. Contourite facies of the Faro Drift, Gulf of Cadiz, in: Stow, D.A.V., Piper, D.J.W. (Eds.), Fine grained sediments: deep-water processes and facies. Geological Society by Blackwell Scientific Publications, Special Publication 15, 275–292.

Hanebuth, T.J.J., Zhang, W., Hofmann, A.L., Löwemark, L.A., Schwenk, T., 2015. Oceanic density fronts steering bottom-current induced sedimentation deduced from a 50 ka contourite-drift record and numerical modeling (off NW Spain). Quaternary Science Reviews 112, 207-225.

Hernández-Molina, F.J., Llave, E., Stow, D.A.V., García, M., Somoza, L., Vázquez, J.T., Lobo, F.J., Maestro, A., Díaz del Río, V., León, R., Medialdea, T., Gardner, J., 2006. The contourite depositional system of the Gulf of Cádiz: A sedimentary model related to the bottom current activity of the Mediterranean outflow water and its interaction with the continental margin. Deep-Sea Research II 53, 1420-1463.

Hernández-Molina, F.J., Bohoyo, F., Naveira Garabato, A., Galindo-Zaldívar, J., Lobo, F.J., Maldonado, A., Rodríguez-Fernández, J., Somoza, L., Stow, D.A.V., Vázquez, J.T., 2007. The Scan Basin evolution: oceanographic consequences of the deep connection between the Weddell and Scotia Seas (Antarctica), in: SCAR (Ed.), 1st International Symposium on Marine Sciences — ISMS07. U.S. Geological Survey and The National Academies, vol. EA086. SCAR, pp. 1–4.

Hernández-Molina, F.J., Llave, E., Stow, D.A.V., 2008a. Continental slope contourites, in: Rebesco, M., Camerlenghi, A. (Eds.), Contourites. Developments in Sedimentology, vol. 60. Elsevier, Amsterdam, pp. 379–407.

Hernández-Molina, F.J., Maldonado, A., Stow, D.A.V., 2008b. Abyssal plain contourites, in: Rebesco, M., Camerlenghi, A. (Eds.), Contourites. Developments in Sedimentology, 60. Elsevier, pp. 347-377.

Hernández-Molina, F.J., Paterlini, M., Violante, R., Marshall, P., de Isasi, M., Somoza, L., Rebesco, M., 2009. Contourite depositional system on the Argentine Slope: an excepcional record of the influence of Antarctic water masses. Geology 37, 507-510.

Hernández-Molina, F.J., Llave, E., Preu, B., Ercilla, G., Fontan, A., Bruno,M., Serra, N., Gomiz, J.J., Brackenridge, R.E., Sierro, F.J., Stow, D.A.V., García,M., Juan, C., Sandoval, N., Arnaiz,A., 2014. Contourite processes associated with the Mediterranean Outflow Water after its exit from the Strait of Gibraltar: global and conceptual implications. Geology 42, 227–230.

Hillenbrand, C.D., Ehrmann,W., 2005. Late Neogene to Quaternary environmental changes in the Antarctic Peninsula region: evidence from drift sediments. Global and Planetary Change 45, 165–191.

Hovland, M., 1984. Gas-induced erosion features in the North Sea. Earth Surface Processes and Landforms 9, 298–228.

Josenhans, H.W., King, L.H., Fader, G.B., 1978. A side-scan sonar mosaic of pockmarks on the Scotian Shelf. Canadian Journal of Earth Sciences 15, 831–840.

Jullion, L., Naveira Garabato, A.C., Bacon, S., Meredith, M.P., Brown, P.J., Torres-Valdés, S., Speer, K.G., Holland, P.R., Dong, J., Bakker, D., Hoppema, M., Loose, B., Venables, H.J., Jenkins, W.J., Messias, M.-J., Fahrbach, E., 2013. The contribution of the Weddell Gyre to the lower limb of the Global Overturning Circulation. Journal of Geophysical Research: Oceans 119, 3357-3377, doi: 10.1002/2013JC009725.

Kuhn, G., Weber, M., 1993. Acoustical characterization of sediments by Parasound and 3.5 kHz systems: related sedimentary processes on the southeastern Weddell Sea continental slope, Antarctica. Marine Geology 113, 201-217.

Laberg, J.S., Camerlenghi, A., 2008. The significance of contourites for submarine stability, in: Rebesco, M., Camerlenghi, A. (Eds.) Contourites, Developments in Sedimentology 60, Elsevier, Amsterdam, pp. 537–556.

Lastras, G., Canals, M., Amblas, D., Frigola, J., Urgeles, R., Calafat, A.M., Acosta, J., 2007. Slope instability along the northeastern Iberian and Balearic continental margins. Geologica Acta 5, 35–47.

Lawver, L.A., Gahagan, L.M., 2003. Evolution of Cenozoic seaways in the circum-Antarctic region. Palaeogeography, Palaeoclimatology, Palaeoecology 198, 11–37.

Legg, S., Briegleb, B., Chang, Y., Chassignet, E.P., Danabasoglu, G., Ezer, T., Gordon, A.L., Griffies, S., Hallberg, R., Jackson, L., Large, W., Ozgokmen, T.M., Peters, H., Price, J., Riemenschneider, U., Wu, W., Xu, X, Yang, J., 2009. Improving oceanic overflow representation in climate models. Bulletin of the American Meteorological Society 90, doi:10.1175/2008BAMS2667.1.

Livermore, R., Hillenbrand, C.D., Meredith, M., Eagles, G., 2007. Drake Passage and Cenozoic climate: an open and shut case? Geochemistry, Geophysics, Geosystems 8, Q01005, doi:10.1029/2005GC001224.

Lobo, F.J., Hernández-Molina, F.J., Bohoyo, F., Galindo-Zaldívar, J., Maldonado, A., Martos, Y., Rodríguez-Fernández, J., Somoza, L., Vázquez, J.T., 2011. Furrows in the southern Scan Basin, Antarctica: interplay between tectonic and oceanographic influences. Geo-Marine Letters 31, 451–464.

Locarnini, R.A., Whitworth III, T., Nowlin Jr., W.D., 1993. The importance of the Scotia Sea on the outflow of Weddell Sea Deep Water. Journal of Marine Research 51, 135–153.

Lodolo, E., Donda, F., Tassone, A., 2006. Correction to “Western Scotia Sea margins: Improved constraints on the opening of the Drake Passage”. Journal of Geophysical Research 111: doi: 10.1029/2006JB004569. issn: 0148-0227.

Lodolo, E., Civile, D., Vuan, A., Tassone, A., Geletti, R., 2010. The Scotia–Antarctica plate boundary from 35°W to 45°W. Earth and Planetary Science Letters 293, 200–215.

Maldonado, A., Zitellini, N., Leitchenkov, G., Balanyá, J.C., Coren, F., Galindo-Zaldívar, J., Lodolo, E., Jabaloy, A., Zanolla, C., Rodríguez-Fernández, J., Vinnikovskaya, O., 1998. Small ocean basin development along the Scotia-Antarctica plate boundary and in the northern Weddell Sea. Tectonophysics 296, 371–402.

Maldonado, A., Barnolas, A., Bohoyo, F., Galindo-Zaldivar, J., Hernández-Molina, J., Lobo, F., Rodríguez-Fernández, J., Somoza, L., Vázquez, J.T., 2003. Contourite deposits in the central Scotia Sea: the importance of the Antarctic Circumpolar Current and the Weddell Gyre flows. Palaeogeography, Palaeoclimatology, Palaeoecology 198, 187–221.

Maldonado, A., Barnolas, A., Bohoyo, F., Escutia, C., Galindo-Zaldivar, J., Hernández- Molina, J., Jabaloy, A., Lobo, F.J., Nelson, C.H., Rodríguez-Fernández, J., Somoza, L., Vázquez, J.T., 2005. Miocene to recent contourite drifts development in the northern Weddell Sea (Antarctica). Global and Planetary Change 45, 99–129.

Maldonado, A., Bohoyo, F., Galindo-Zaldívar, J., Hernández-Molina, F.J., Jabaloy, A., Lobo, F.J., Rodríguez-Fernández, J., Suriñach, E., Vázquez, J.T., 2006. Ocean basins near the Scotia–Antarctic plate boundary: influence of tectonics and paleoceanography on the Cenozoic deposits. Marine Geophysical Researches 27, 83–107.

Maldonado, M., Bohoyo, F., Galindo-Zaldívar, J., Hernández-Molina, F.J., Lobo, F.J., Lodolo, E., Martos, Y.M., Pérez, L.F., Schreider, A.A., Somoza, L., 2014. A model of oceanic development by ridge jumping: opening of the Scotia Sea. Global and Planetary Change 123, 152–173.

Maldonado, A., Dalziel, I.W.D., Leat, P.T., 2015. The global relevance of the Scotia Arc: An introduction. Global and Planetary Change 125, A1–A8.

McCave, I.N., Carter, L., 1997. Sedimentation beneath the Deep Western Boundary Current o¡ northern New Zealand. Deep-Sea Researches 44, 1203–1237.

McCave, I.N., Tucholke, B.E., 1986. Deep current-controlled sedimentation in the western North Atlantic, in: Vogt, P.R., Tucholke, B.E. (Eds.), The Geology of North America, Vol. M The Western North Atlantic Region. Geological Society of America, Boulder, pp. 1117–1126.

Mézerais, M.-L., Faugères, J.-C., Figueiredo Jr., A.G., Massé, L., 1993. Contour current accumulation off the Vema Channel mouth, southern Brazil Basin: pattern of a “contourite fan”. Sedimentary Geology 82, 173–187.

Morozov, E.G., Demidov, A.N., Tarakanov, R.Y., Zenk, W., 2010. Abyssal Channels in the Atlantic Ocean. Water Structure and Flows. Springer, ISBN: 978-90-481-9357-8.

Mougenot, D., Vanney, J.R., 1982. Les rides de contourites Plio-Quaternaires de la pente continentale sud-portugaise. Bulletin de l'Institut de géologie du bassin d'Aquitaine 31,131–139m

Naveira Garabato, A.C., Heywood, K.J., Stevens, D.P., 2002a. Modification and pathways of Southern Ocean Deep Waters in the Scotia Sea. Deep Sea Research Part I: Oceanographic Research Papers 49, 681–705.

Naveira Garabato, A.C., McDonagh, E.L., Stevens, D.P., Heywood, K.J., Sanders, R.J., 2002b. On the export of Antarctic Bottom Water from the Weddell Sea. Deep Sea Research Part II: Topical Studies in Oceanography 49, 4715–4742.

Orsi, A.H., Johnson, G.C., Bullister, J.L., 1999. Circulation, mixing, and production of Antarctic Bottom Water. Progress in Oceanography 43, 55–109.

Palmer, M., Gomis, D., Flexas, M.M., Jordá, G., Jullion, L., Tsubouchi, T., Naveira Garabato, A.C., 2012. Water mass pathways and transports over the South Scotia Ridge west of 50ºC. Deep-Sea Research I 59, 8–24.

Payton, C.E., 1977. Seismic Stratigraphy- applications to hydrocarbon exploration. American Association of Petroleum Geologists Memoirs, 26.

Pedlosky, J., 1996. Ocean circulation Theory. Springer Science & Business Media, Science.

Pérez, L.F., Lodolo, E., Maldonado, A., Hernandez-Molina, F.J., Bohoyo, F., Galindo-Zaldivar, J., Lobo, F.J., Burca, M., 2014a. Tectonic development, sedimentation and paleoceanography of the Scan Basin (southern Scotia Sea, Antarctica). Global and Planetary Change 123, 344–358.

Pérez., L.F., Maldonado, A., Bohoyo, F., Hernández-Molina, F.J., Vázquez, J.T., Lobo, F.J., Martos, Y.M., 2014b. Depositional processes and growth patterns of isolated oceanic basins: the Protector and Pirie basins of the Southern Scotia Sea (Antarctica). Marine Geology 357, 163–181.

Plaza-Faverola, A., Westbrook, G.K., Ker, S., Exley, R.J.K., Gailler, A., Minshull, T.A., Broto, K., 2010. Evidence from three-dimensional seismic tomography for a substantial accumulation of gas hydrate in a fluid-escape chimney in the Nyegga pockmark field, offshore Norway. Journal of Geophysical Research 115, B08104, doi:10.1029/2009JB007078

Preu, B., Hernández-Molina, F.J., Violante, R., Piola, A.R., Paterlini, C.M., Schwenk, T., Voigt, I., Krastel, S., Spiess, V., 2013, Morphosedimentary and hydrographic features of the northern Argentine margin: The interplay between erosive, depositional and gravitational processes and its conceptual implications. Deep-Sea Research I 75, 157–174.

Rebesco, M., Camerlenghi, A. (eds.) 2008. Contourites. Developments in Sedimentology 60. Elsevier.

Rebesco, M., Stow, D.A.V., 2001. Seismic expression of contourites and related deposits: a preface. Marine Geophysical Research 22, 303–308.

Rebesco, M., Hernández-Molina, F.J., Van Rooij, D.,Wåhlin, A., 2014. Contourites and associated sediments controlled by deep-water circulation processes: state of the art and future considerations. Marine Geology 352, 111–154.

Reed, D.L., Meyer, A.W., Silver, E.A., Prasetyo, H., 1987. Contourite sedimentation in an intraoceanic forearc system: eastern Sunda Arc, Indonesia. Marine Geology, 76, 223–242.

Roberts, D.G., Hogg, N.G., Derek, G., Bishop, G., Flewellen, C.G., 1974. Sediment distribution around moated seamounts in the Rockall Trough. Deep-Sea Research Part A 21, 175–184.

Ruano, P., Bohoyo, F., Galindo-Zaldívar, J., Pérez, L.F., Hernández-Molina, F.J., Maldonado, A., García, M., Medialdea, T., 2014. Mass transport processes in the southern Scotia Sea: Evidence of paleoearthquakes. Global and Planetary Change 123, 374-391.

Ryan, W.B.F., Carbotte, S.M., Coplan, J., O'Hara, S., Melkonian, A., Arko, R., Weissel, R.A., Ferrini, V., Goodwillie, A., Nitsche, F., Bonczkowski, J., Zemsky, R., 2009. Global Multi-Resolution Topography (GMRT) synthesis data set, Geochemistry, Geophysics, Geosystems *10, Q03014*, doi:10.1029/2008GC002332.

Schodlok, M.P., Hellmer, H.H., Beckmann, A., 2002. On the transport, variability and origin of dense water masses crossing the SSR. Deep-Sea Research II 49, 4807–4825.

Smith, W.H.F., Sandwell, D.T., 1997. Global seafloor topography from satellite altimetry and ship depth soundings. Science 277, 1957–1962.

Somoza, L., León, R., Medialdea, T., Pérez, L.F., González, F.J., Maldonado, A., 2014. Seafloor mounds, craters and depressions linked to seismic chimneys breaching fossilized diagenetic bottom simulating reflectors in the central and southern Scotia Sea, Antarctica. Global and Planetary Change 123, 359-373.

Speer, K., Rintoul, S.R., Sloyan, B., 2000. The diabatic Deacon Cell. Journal of Physycal Oceanography 30, 3212–3222.

Stoker, M.S., Akhurst, M.C., Howe, J.A., Stow, D.A.V., 1998. Sediment drifts and contourites on the continental margin off northwest Britain. Sedimentary Geology 115, 33–51.

Stow, D.A.V., Faugeres, J.C., Howe, J.A., Pudsey, C.J., Viana, A.R., 2002. Bottom currents, contourites and deep sea sediment drifts: current state-of-the-art. Geological Society of London Memoirs 22, 7–20.

Stow, D.A.V., Hernández-Molina, F.J., Llave, E., Sayago, M., Díaz del Río, V., Branson, A., 2009. Bedform-velocity matrix: the estimation of bottom current velocity from bedform observations. Geology 37, 327–330.

Tarakanov, R.Y., 2009. Antarctic bottom water in the Scotia Sea and the Drake Passage. Oceanology 49, 607–621.

Tarakanov, R.Y., 2010. Circumpolar Bottom Water in the Scotia Sea and Drake Passage. Oceanology 50, 5–22.

Tarakanov, R.Y., 2012. The Scotia Sea and the Drake Passage as an Orographic Barrier for the Antarctic Circumpolar Current. Oceanology 52, 157–170.

Veeken, C.H., 2007. Seismic Stratigraphy, Basin Analysis and Reservoir Characterisation. Handbook of Geophysical Exploration, Volume 37. Elsevier, Amsterdam.

Vuan, A., Lodolo, E., Panza, G.F., Sauli, C., 2005. Crustal structure beneath Discovery Bank in the Scotia Sea from group velocity tomography and seismic reflection data. Antarctic Science 17, 97-106.

Wynn and Stow, 2002 Wynn, R.B., Stow, D.A.V., 2002. Classification and characterization of deep-water sediment waves. Marine Geology 192, 7-22.

FIGURE CAPTIONS

Figure 1. Study area. a) Regional bathymetry of the Scotia Sea region, showing the small basins connecting the Weddell Sea with the Scotia Sea and the location of Scan Basin at the eastern extreme of the southern Scotia Sea. Source: Smith and Sandwell, 1997. b) Detailed bathymetry of Scan Basin, limited by Bruce and Discovery banks, divided by a gap into a northern and a southern block. Source of data: Marine Geoscience Data System (Ryan et al., 2009).

Figure 2. Oceanographic characterization of the Scan Basin region. a) Water masses and general circulation patterns, illustrating the direction of flow of the CBW, WDW, and WSDW. Modified from Morozov et al. (2010). b) Transversal profile across Bruce Passage showing the vertical distribution of flow velocity and the distribution of water masses with depth. Modified from Naveira-Garabato et al. (2002).

Figure 3: Acoustic facies characterization of Scan Basin. a) Facies distribution map showing the location of selected profiles. b) to f) TOPAS profiles illustrating the characteristics of the non-penetrative, stratified, and transparent acoustic facies identified in this study.

Figure 4. Morphological map showing the distribution of the erosional, depositional, gravitational, volcanic and fluid-escape-related morphological features identified in Scan Basin.

Figure 5. Morphological characteristics of erosional features (lineations, furrows and channels) and depositional features (sheeted deposits, sediment waves and mounded deposits). Figure 5a shows the locations of the TOPAS profiles and detailed bathymetric maps displayed in Figs. 5, 7 and 10. Please note that horizontal scale varies between profiles.

Figure 6. Morphological characteristics of erosional (channels) and depositional (stratified deposits and mounded bodies) features in Scan Basin. The location of profiles and bathymetric detailed map are shown in Fig. 5a.

Figure 7. Morphological characterization of mass-wasting (bodies of transparent facies and scarps) and fluid-escape-related features (craters). The location of the bathymetric

map in 7a is shown in Fig. 5a. Figure 7d shows a morphological interpretation of these features on the Discovery Bank terrace (see location in Fig. 7a).

Figure 8. Seismic stratigraphic characterization of the Scan Basin abyssal plain. a) and b) TOPAS profile from this study superposed on a multichannel seismic profile from Scan basin that shows the seismic units and age attribution at a basin scale, modified from Pérez et al. (2014a). b) shows the seismic units U1 to U5 defined in this work. c) Isochore maps of each seismic unit. d) and e) Main characteristics of the seismic units in TOPAS profiles. Profile location is shown in Fig. 8c.

Figure 9. a) Morphological characterization of Discovery Bank (location shown in Fig. 7a) showing the distribution of craters and slide scars and the inferred distribution of craters evolved into scars. b) Detailed bathymetric map illustrating the morphological correlation between craters and slide scars.

Figure 10. Schematic diagram of the circulation pattern inferred from the study of the Scan Basin and Discovery Bank CDS features. It includes a northward WSDW flow close to Bruce Bank, a weak recirculation close to Discovery Bank and the eastward-north-eastward flow of the CBW/WDW associated to the AAC.

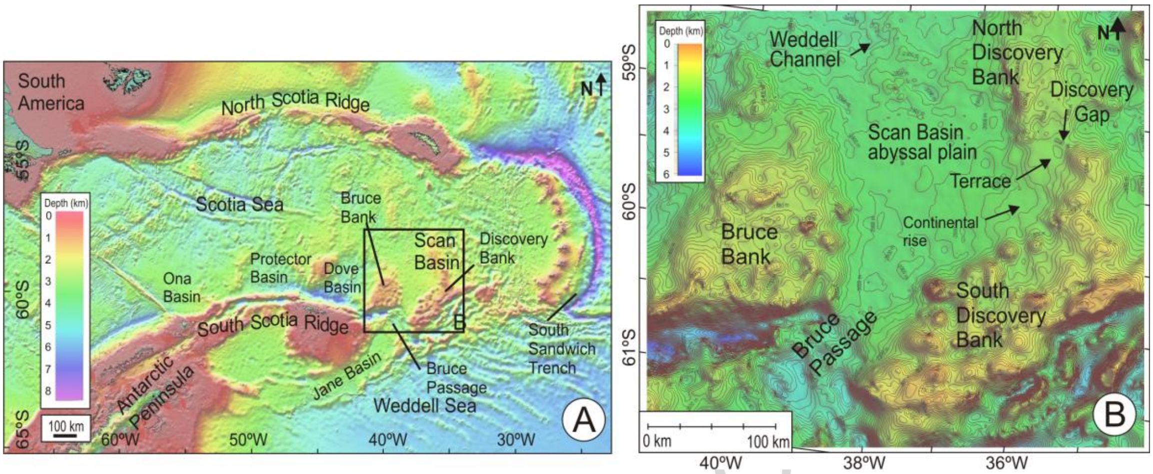
South America
North Scotia Ridge
Scotia Sea
Bruce Bank
Scan Basin
Discovery Bank
Protector Basin
Dove Basin
Ona Basin
South Scotia Ridge
Antarctic Peninsula
Jane Basin
Bruce Passage
Weddell Sea
South Sandwich Trench
Depth (km)
100 km
55°S
60°S
65°S
60°W
50°W
40°W
30°W
A
B
Weddell Channel
North Discovery Bank
Discovery Gap
Scan Basin abyssal plain
Terrace
Continental rise
Bruce Bank
Bruce Passage
South Discovery Bank
0 km
100 km
59°S
60°S
61°S
40°W
38°W
36°W

Figure 1

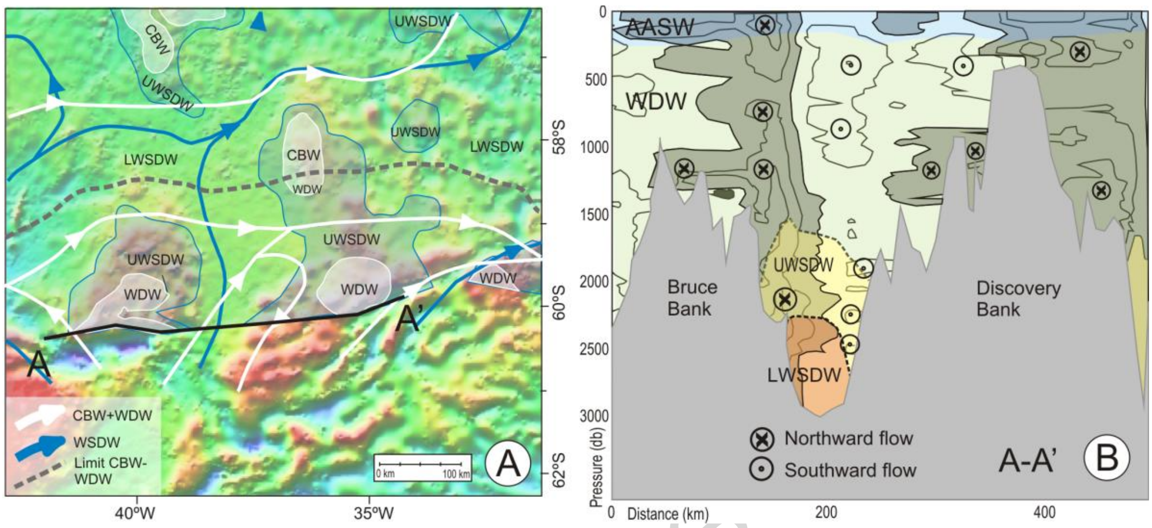
CBW
UWSDW
UWSDW
CBW
WDW
UWSDW
LWSDW
LWSDW
UWSDW
WDW
UWSDW
WDW
WDW
A
A'
CBW+WDW
WSDW
Limit CBW-WDW
0 km 100 km
A
40ºW
35ºW
58ºS
60ºS
62ºS
AASW
WDW
Bruce Bank
UWSDW
LWSDW
Discovery Bank
Northward flow
Southward flow
A-A'
B
Pressure (db)
Distance (km)
0
500
1000
1500
2000
2500
3000
0
200
400

Figure 2

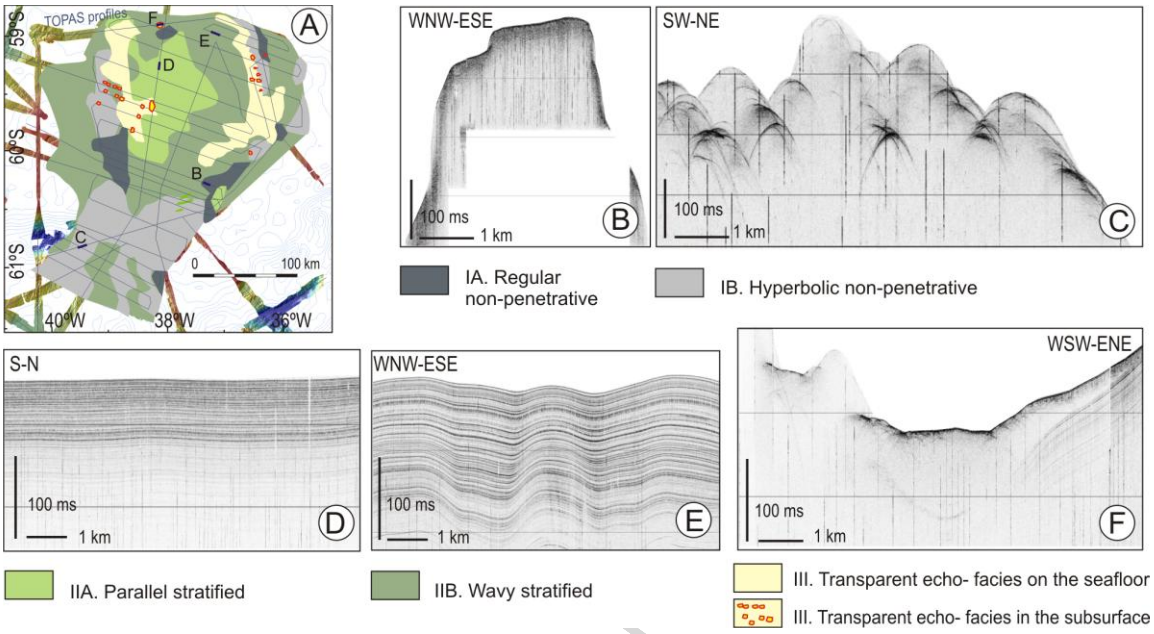
TOPAS profiles
59°S
60°S
61°S
40°W
38°W
36°W
0
100 km
A
B
C
D
E
F
WNW-ESE
100 ms
1 km
SW-NE
IA. Regular non-penetrative
IB. Hyperbolic non-penetrative
S-N
WSW-ENE
IIA. Parallel stratified
IIB. Wavy stratified
III. Transparent echo- facies on the seafloor
III. Transparent echo- facies in the subsurface

Figure 3

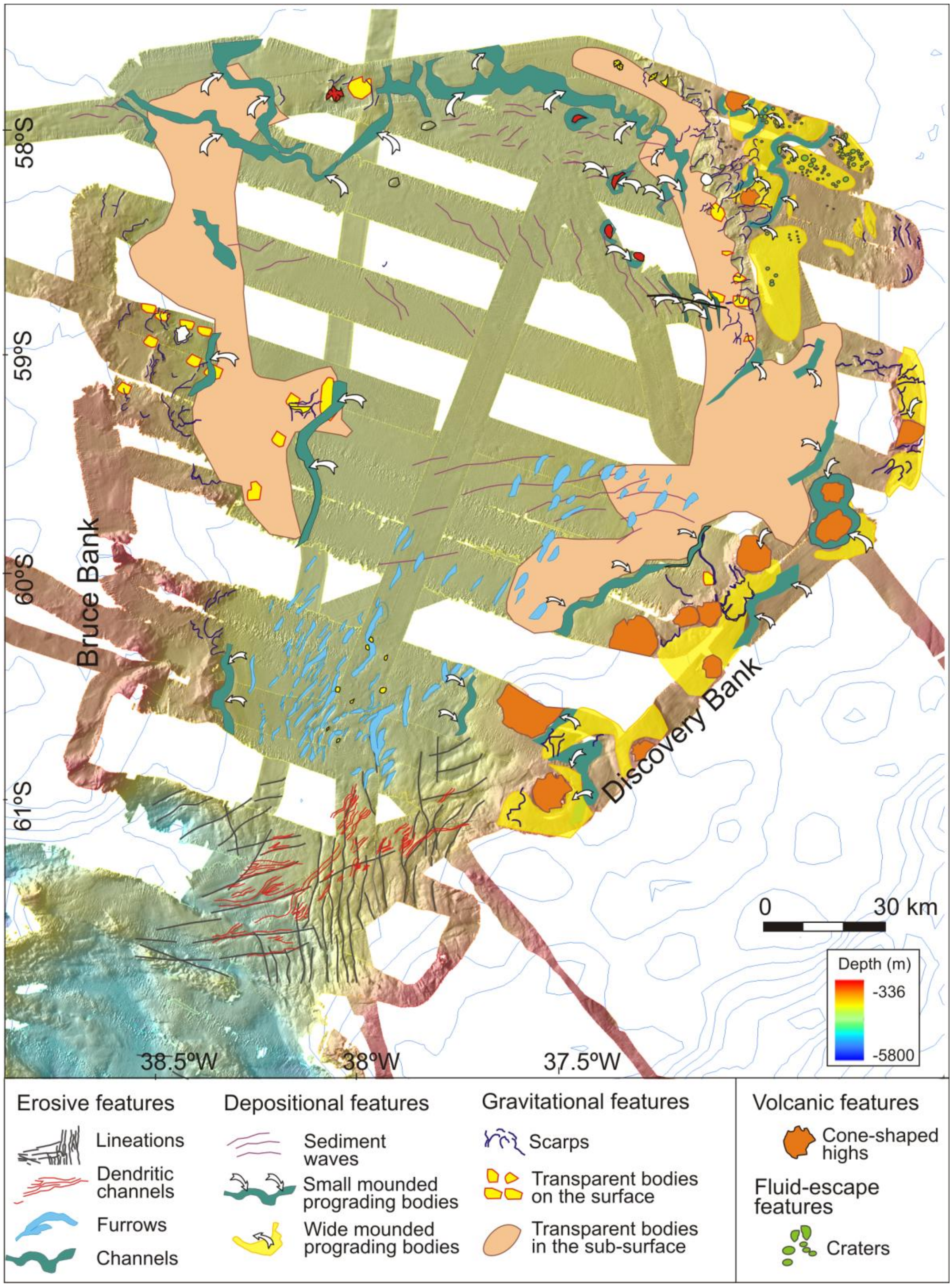
58°S
59°S
60°S
61°S
Bruce Bank
Discovery Bank
38.5°W
38°W
37.5°W
0
30 km
Depth (m)
-336
-5800
Erosive features
Lineations
Dendritic channels
Furrows
Channels
Depositional features
Sediment waves
Small mounded prograding bodies
Wide mounded prograding bodies
Gravitational features
Scarps
Transparent bodies on the surface
Transparent bodies in the sub-surface
Volcanic features
Cone-shaped highs
Fluid-escape features
Craters

Figure 4

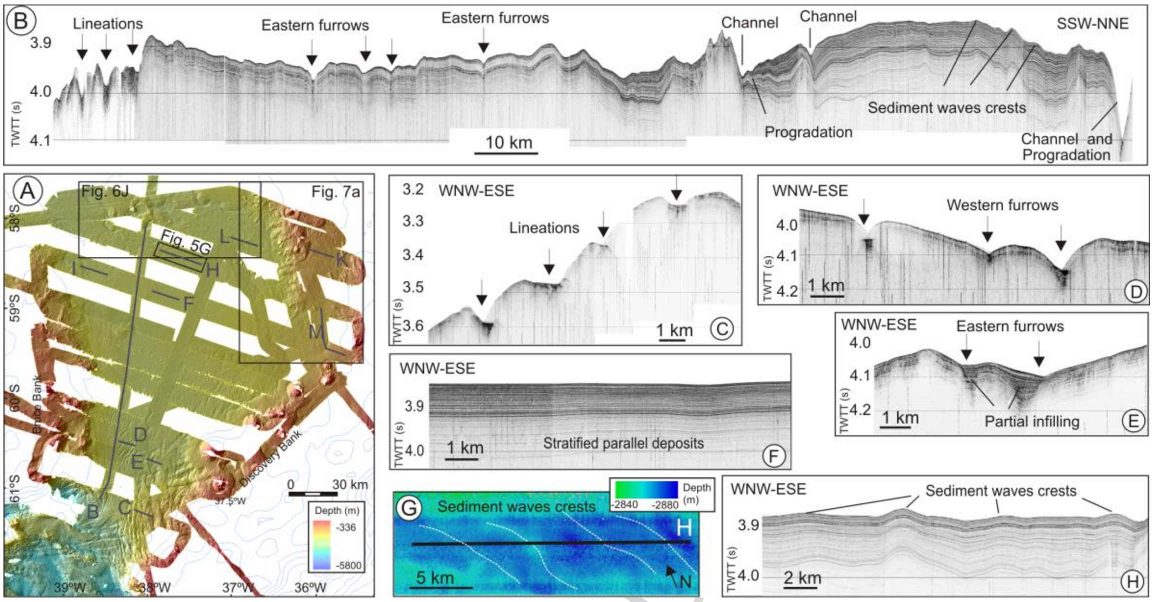

B
Lineations
Eastern furrows
Eastern furrows
Channel
Channel
SSW-NNE
Sediment waves crests
Progradation
Channel and Progradation
10 km
TWTT (s)
A
Fig. 6J
Fig. 7a
Fig. 5G
Discovery Bank
30 km
Depth (m)
-336
-5800
39ºW
38ºW
37ºW
36ºW
WNW-ESE
Lineations
1 km
C
Western furrows
D
Eastern furrows
Partial infilling
E
Stratified parallel deposits
F
G
Sediment waves crests
5 km
Sediment waves crests
2 km
H

Figure 5

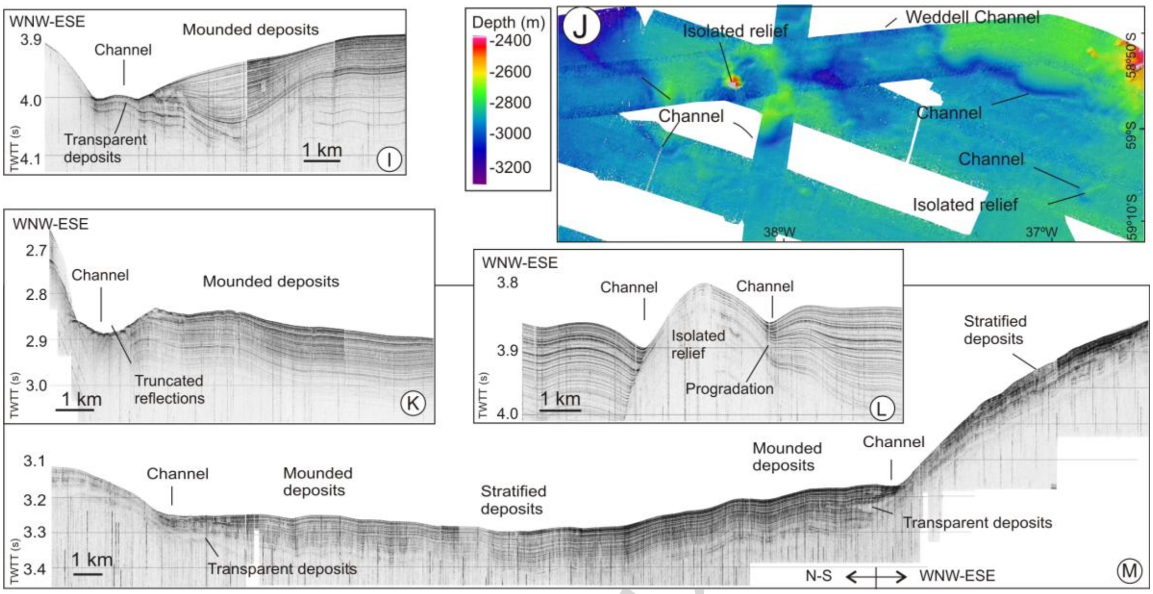

WNW-ESE
Mounded deposits
Channel
Transparent deposits
1 km
TWTT (s)
3.9
4.0
4.1
I
Depth (m)
-2400
-2600
-2800
-3000
-3200
J
Isolated relief
Weddell Channel
Channel
Channel
Channel
Isolated relief
58°50'S
59°S
59°10'S
38°W
37°W
WNW-ESE
2.7
2.8
2.9
3.0
Channel
Mounded deposits
Truncated reflections
1 km
K
WNW-ESE
3.8
3.9
4.0
Channel
Channel
Isolated relief
Progradation
1 km
L
Stratified deposits
3.1
3.2
3.3
3.4
Channel
Mounded deposits
Stratified deposits
Mounded deposits
Channel
Transparent deposits
Transparent deposits
1 km
N-S
WNW-ESE
M

Figure 6

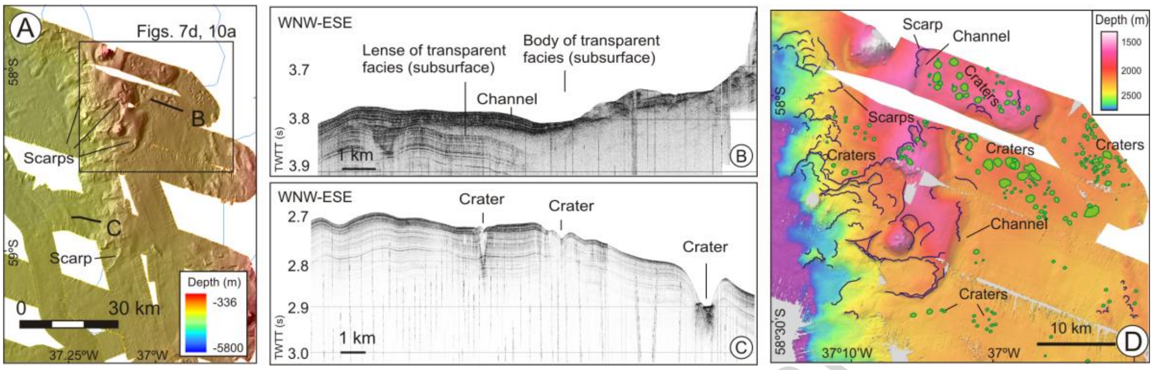

A
Figs. 7d, 10a
58°S
B
Scarps
C
59°S
Scarp
Depth (m)
-336
-5800
0
30 km
37.25°W
37°W
WNW-ESE
Lense of transparent facies (subsurface)
Body of transparent facies (subsurface)
Channel
3.7
3.8
3.9
TWTT (s)
1 km
B
WNW-ESE
Crater
Crater
Crater
2.7
2.8
2.9
3.0
TWTT (s)
1 km
C
Scarp
Channel
Depth (m)
1500
2000
2500
Craters
Scarps
Craters
Craters
Craters
Channel
Craters
58°S
58°30'S
37°10'W
37°W
10 km
D

Figure 7

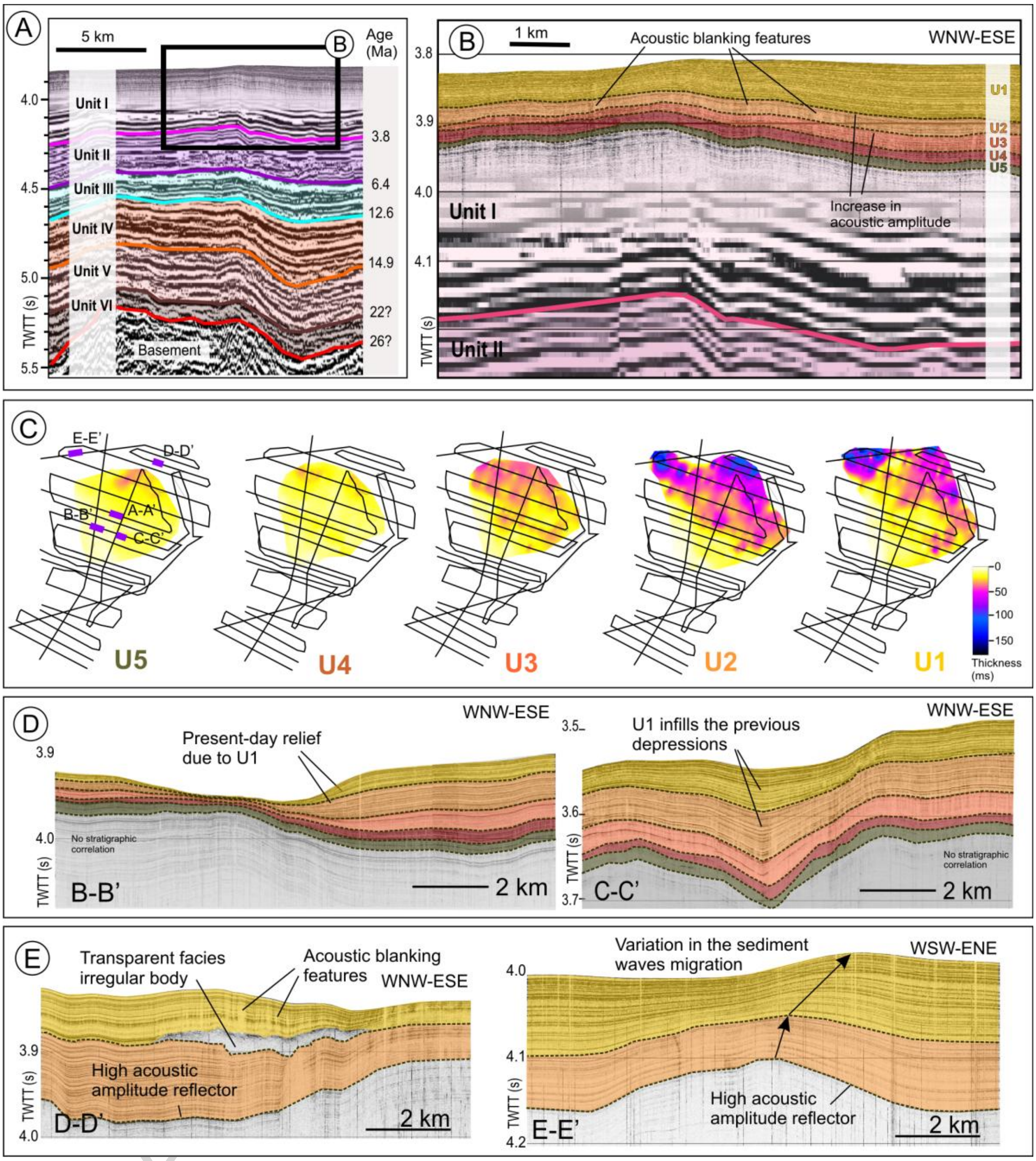
A
5 km
B
Age (Ma)
Unit I
Unit II
Unit III
Unit IV
Unit V
Unit VI
Basement
3.8
6.4
12.6
14.9
22?
26?
TWTT (s)
1 km
Acoustic blanking features
WNW-ESE
U1
U2
U3
U4
U5
Increase in acoustic amplitude
C
E-E'
D-D'
A-A'
B-B'
C-C'
U5
U4
U3
U2
U1
Thickness (ms)
D
Present-day relief due to U1
No stratigraphic correlation
B-B'
2 km
U1 infills the previous depressions
C-C'
E
Transparent facies irregular body
Acoustic blanking features
High acoustic amplitude reflector
D-D'
Variation in the sediment waves migration
WSW-ENE
E-E'

Figure 8

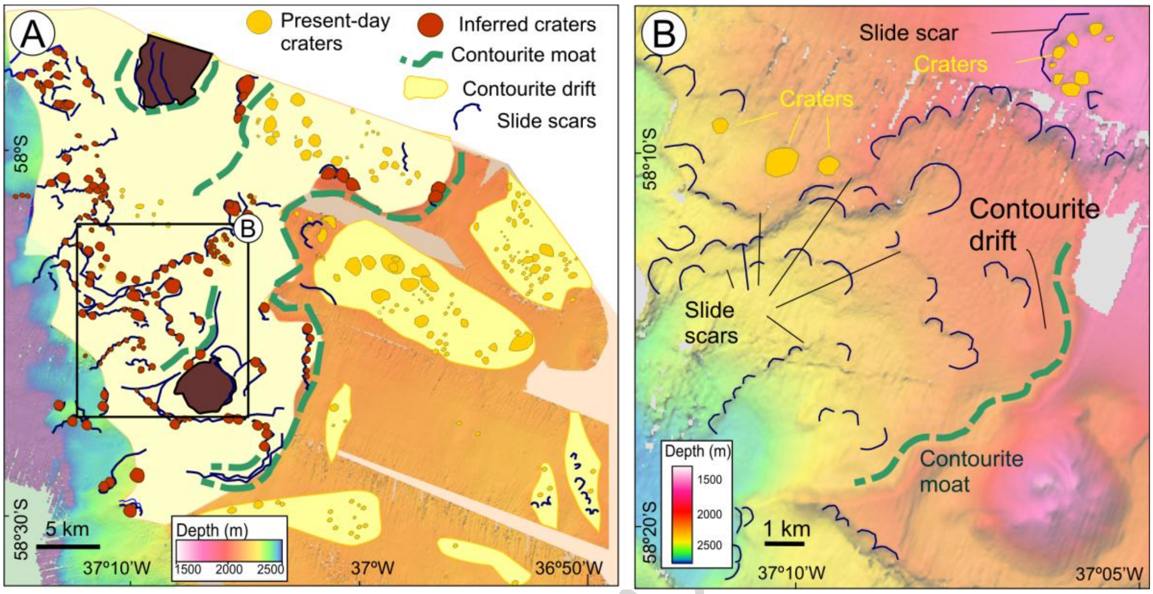
A
Present-day craters
Inferred craters
Contourite moat
Contourite drift
Slide scars
58°S
58°30'S
5 km
Depth (m)
1500 2000 2500
37°10'W
37°W
36°50'W
B
Slide scar
Craters
Craters
58°10'S
Contourite drift
Slide scars
Contourite moat
Depth (m)
1500
2000
2500
58°20'S
1 km
37°10'W
37°05'W

Figure 9

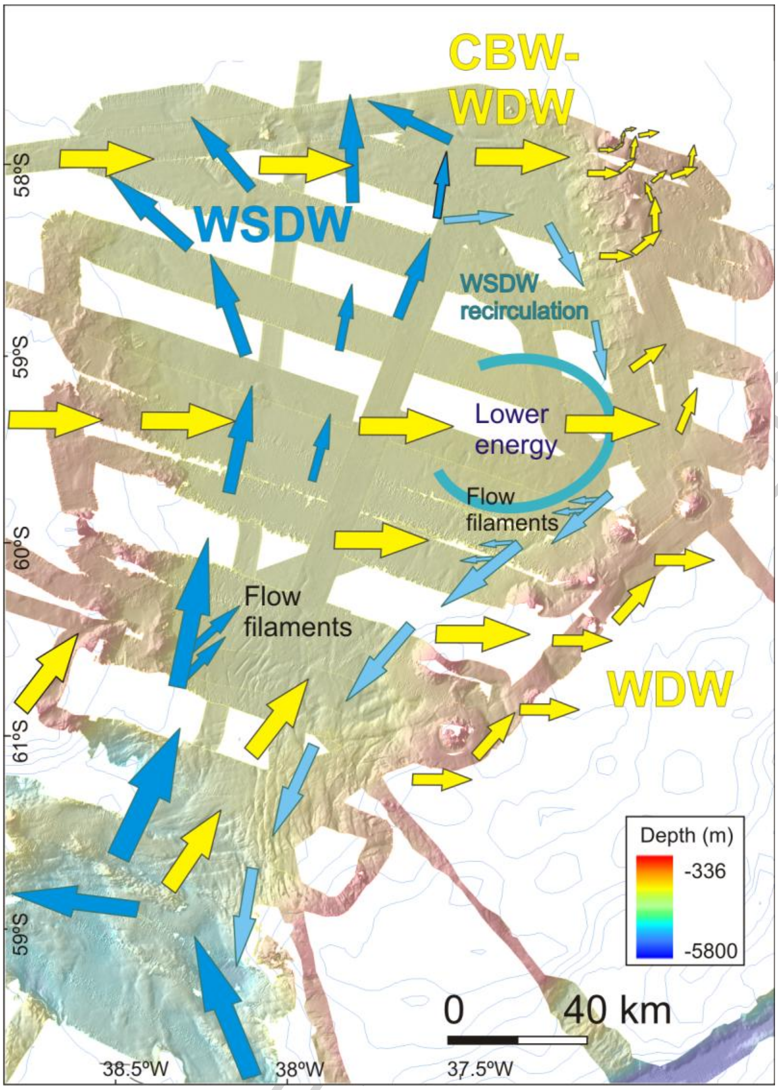
CBW-
WDW
WSDW
WSDW
recirculation
Lower
energy
Flow
filaments
Flow
filaments
WDW
Depth (m)
-336
-5800
0
40 km
58°S
59°S
60°S
61°S
59°S
38.5°W
38°W
37.5°W

Figure 10